Modalities of Distortion of Physiological Voltage Signals by Patch-Clamp Amplifiers: A Modeling Study

Jacopo Magistretti,* Massimo Mantegazza,* Marco de Curtis,* and Enzo Wanke#
*Laboratorio di Neurofisiologia Sperimentale, Istituto Nazionale Neurologico "Carlo Besta," and #Dipartimento di Fisiologia Generale e Biochimica, Laboratorio di Elettrofisiologia, Università di Milano, Milan, Italy

ABSTRACT An extensive evaluation of the possible alterations affecting physiological voltage signals recorded with patch-clamp amplifiers (PCAs) working in the current-clamp (CC) mode was carried out by following a modeling approach. The PCA output voltage and current signals obtained during CC recordings performed under simplified experimental conditions were exploited to determine the equations describing the generation of error currents and voltage distortions by PCAs. The functions thus obtained were used to construct models of PCAs working in the CC mode, which were coupled to numerical simulations of neuronal bioelectrical behavior; this allowed us to evaluate the effects of the same PCAs on different physiological membrane-voltage events. The models revealed that rapid signals such as fast action potentials are preferentially affected, whereas slower events, such as low-threshold spikes, are less altered. Prominent effects of model PCAs on fast action potentials were alterations of their amplitude, duration, depolarization and repolarization speeds, and, most notably, the generation of spurious afterhyperpolarizations. Processes like regular firing and burst firing could also be altered, under particular conditions, by the model PCAs. When a cell consisting of more than one single intracellular compartment was considered, the model PCAs distorted fast equalization transients. Furthermore, the effects of different experimental and cellular parameters (series resistance, cell capacitance, temperature) on PCA-generated artifacts were analyzed. Finally, the simulations indicated that no off-line correction based on manipulations of the error-current signals returned by the PCAs can be successfully performed in the attempt to recover unperturbed voltage signals, because of alterations of the overall current flowing through the cell-PCA system.

INTRODUCTION

The whole-cell variant of the patch-clamp technique is currently widely applied, and is used for recording not only cell currents in the voltage-clamp mode, but also membrane voltage in current-clamp (CC) conditions. Membrane-voltage events that have been recorded and studied in different cell systems with patch-clamp amplifiers (PCAs) include fast and slow action potentials (APs) (Johansson et al., 1992; Sontheimer et al., 1992; D'Angelo et al., 1995; Zhang and McBain, 1995; Gryder and Coulter, 1996), various types of afterhyperpolarization (Kawaguchi, 1993; Zhang and McBain, 1995; Sciancalepore and Constanti, 1995; Gryder and Coulter, 1996), repetitive and burst firing (Stern et al., 1992; Bielefeldt and Jackson, 1993; Kawaguchi, 1993; Pape et al., 1994; D'Angelo et al., 1995), and passive voltage transients reflecting charge movements between cell compartments (D'Angelo et al., 1993). However, it has recently been demonstrated experimentally that rapid voltage signals, such as APs, can be remarkably distorted when recorded with conventional PCAs in the CC mode, rather than classical voltage followers (Magistretti et al., 1996). Moreover, when perturbed, rapid voltage signals are observed at the PCA voltage output, significant and otherwise unexpected current signals are simultaneously returned by the PCA current output, which correspond to error currents (I_Es) improperly flowing through the amplifier itself. The generation of I_Es by PCAs used in the CC mode is a consequence of the electronic design of their headstage, which is essentially a current-to-voltage converter of very low (ideally zero) input resistance, especially conceived for low-series-resistance voltage-clamp recordings; the conversion of such a unit into a voltage-recording device is accomplished by introducing additional feedback circuits that improve the basically very low PCA input-stage resistance, but only to a limited extent (see Magistretti et al., 1996). PCA-driven I_Es, in turn, can distort otherwise unperturbed physiological voltage signals in two ways: 1) by causing a voltage drop across the cell-to-amplifier series resistance, and 2) by altering the amount of current actually charging the membrane capacitance. Under simplified experimental conditions, namely when examining passive model-cell circuits into which known command-current waveforms are supplied, the entity of the voltage error thus introduced and returned by the PCA can be directly correlated with, and predicted from, the I_E flowing through the PCA itself (Magistretti et al., 1996). These findings raise a number of questions concerning CC recordings made with PCAs, particularly the following:

1. Specifically, what kind of physiological membrane-voltage events are likely to be significantly distorted by conventional PCAs?

2. What are the physiological parameters and experimental conditions that can affect the importance of the distortions generated by PCAs in CC recordings?

Received for publication 27 June 1997 and in final form 4 November 1997.

Address reprint requests to Dr. Jacopo Magistretti, Laboratorio di Neurofisiologia Sperimentale, Istituto Nazionale Neurologico "Carlo Besta," Via Celoria 11, 20133 Milano, Italy. Tel.: +39-2-2394296; Fax: +39-2-70600775; E-mail: neurofis@tin.it.

0006-3495/98/02/831/12 $2.00

3. To what extent are the CC data obtained with conventional PCAs susceptible to criticism?

4. In principle, is it possible to carry out reliable off-line corrections of PCA-generated voltage distortions by exploiting the I_E signals returned by the PCA themselves?

The extensive evaluation of such problems with real cells, by comparing recordings obtained from the same cells using either a conventional PCA or a classical voltage follower, would be troublesome and subject to experimental uncertainties. Therefore we addressed the above issues by modeling PCAs working in the CC mode. We were able to derive empirically the transfer functions governing the relationships between input voltage and I_E for three extensively used commercial PCAs (Axopatch 1D, Axopatch 200A, and List EPC-7), and thereby analytically and numerically describe the behavior of both the voltage and current outputs of these instruments under CC conditions. Then we made a simulated PCA interact with model cells endowed with "standard" neuronal membrane-conductance outfits, thereby evaluating the effects of PCA-driven I_Es, under various conditions, on membrane-voltage events such as fast APs, repetitive firing, low-threshold spikes, and burst firing. We also examined the distortions generated by PCAs on passive time constants in a two-compartment cell model. Finally, we resorted to our simulation data to evaluate the feasibility of off-line voltage corrections, based on manipulations on recorded I_Es, in real cellular systems. Our results indicate that conventional PCAs can generate distortions of most rapid membrane-voltage events under a variety of experimental situations; that these distortions are often far from negligible; and that severe intrinsic limitations exist that virtually exclude the possibility of safely performing off-line voltage corrections in real-cell recordings.

METHODS AND THEORY

Measurement and description of PCA-generated voltage distortions and error currents

Evidence has previously been provided that membrane-voltage (V_m) distortions observed in CC recordings made with PCAs are the direct consequence of error-current (I_E) flow through PCAs themselves (Magistretti et al., 1996). In the present study three commercial PCA models in particular were considered, namely Axopatch 1D and 200A (Axon Instruments, Foster City, CA) and EPC-7 (List Electronics, Darmstadt, Germany). To infer the law that governs the generation of I_Es by these PCAs when working in the CC mode, we resorted to a simplified experimental system: we used passive test circuits of the type depicted in Fig. 1 *A*, analogous to a cell membrane. Each consisted of a 500-MΩ resistor (R_{inj}) in series with a capacitor (C_m, the equivalent of cell capacitance) connected to ground. The node between R_{inj} and C_m (node N) was connected, through a second resistor (R_s, the equivalent of series resistance), to the PCA-headstage input; the opposite end of R_{inj} (terminal T) was connected to an external voltage source. The PCA was kept in the CC mode with command current and all compensations set to zero, and, upon commanding a 1.4-ms voltage step at terminal T, the current and voltage responses at the respective PCA outputs were recorded, both at full band; 20–50 traces were acquired and averaged. Recordings were performed at room temperature (22°C). The applied voltage command is expected to charge the circuit capacitance according to a known time law (Fig. 1 *Ba* and *c*, *continuous lines*). The signal returned by the voltage output (V_{out}) of the PCAs displayed significant deviations from the response theoretically predicted at node N (Fig. 1 *Ba* and *c*, *dotted lines*). Moreover, the PCA current output (I_{out}) returned a signal (Fig. 1, *Bb* and *d*), which would not be expected in an unperturbed situation, and which has previously been demonstrated to coincide with the I_E flowing through the PCA (Magistretti et al., 1996).

We found that by summing the integral over time of I_E, and the double integral over time of I_E, each suitably scaled, a trace could be obtained that was virtually indistinguishable from the voltage signal returned by V_{out} (Fig. 1, *Ba* and *c*, *dashed lines*). This observation was verified for all of the investigated PCAs and was confirmed using two different test circuits (see Fig. 1 *legend*). Moreover, the same kind of relationship was found between the I_E and V_{out} signals recorded during action-potential (AP) firing by real neurons (not shown). On the basis of these findings we can write

$$V_{out} = V_C + V_J = 1/C_a \cdot \int I_E \cdot dt + 1/J_a \cdot \int\int I_E \cdot dt^2 \quad (1)$$

and, conversely,

$$I_E = C_a \cdot dV_C/dt = J_a \cdot d^2V_J/dt^2 \quad (2)$$

where C_a and J_a are appropriate proportionality constants. Hence the PCA working in the CC mode can be modeled as being constituted of two elements in series, namely a capacitor of capacitance C_a, and a second element that passes a current proportional to the second time derivative of the potential difference across itself. In the above equations, V_C and V_J are the potential differences across these two elements.

The actual values of the two parameters, C_a and J_a, influence the specific behavior of each PCA model. We found C_a and J_a values of 11.24 pF and 2.64 pF · ms in Ap1D, and of 502.0 pF and 0.643 pF · ms in EPC7 (averages of four independent measurements). As for Ap200A (not shown in Fig. 1 *B*), its behavior in the I_{normal} mode (I_n-Ap200A) was essentially identical to that of Ap1D, whereas in the I_{fast} mode (I_f-Ap200A) C_a and J_a were 1.11 pF and 3.65 pF · ms, respectively.

The considered PCAs were thus modeled according to Eq. 2, the scheme of Fig. 1 *C*, and the empirically derived values of C_a and J_a. On these bases, computer simulations of the experimental protocol applied, as described at the beginning of this paragraph, to the "cell-PCA" system were carried out (see below for details on the simulation meth-

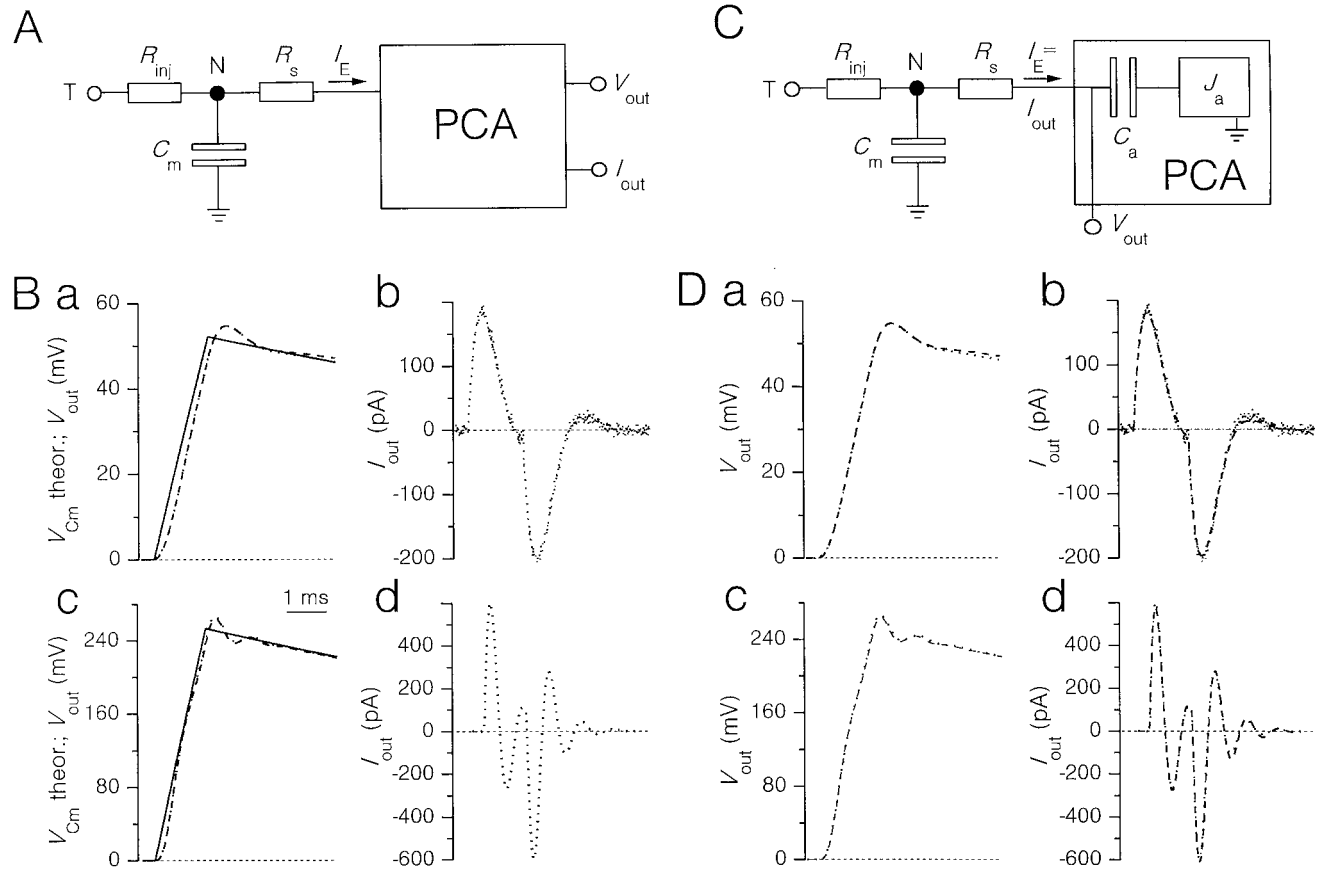

FIGURE 1 Reconstruction of PCA input voltage-to-I_E transfer function. (*A*) Scheme of the test circuits used to measure PCA-generated voltage distortions and error currents. The circuits were connected to the PCA-headstage input. (*B*) Dotted lines are the voltage (*a* and *c*) and current (*b* and *d*) outputs returned by Ap1D (*a* and *b*) and EPC7 (*c* and *d*) in response to the application of a 1.4-ms voltage pulse of 1 V (*a* and *b*) or 5 V (*c* and *d*) at terminal T (see *A*). In the test circuit used in the examples illustrated here, R_{inj}, C_m, and R_s were 500 MΩ, 50 pF, and 30 MΩ, respectively. Continuous lines are the voltage responses theoretically predicted at node N in an unperturbed situation. Dashed lines (largely indistinguishable from the dotted lines) are the voltage traces reconstructed from the output currents by applying Eq. 1 (see text), with C_a and J_a equal to 13.5 pF and 3.06 pF · ms, respectively (in *a*), and to 502.0 pF and 0.643 pF · ms, respectively (in *c*). Another test circuit was also used, in which R_{inj}, C_m, and R_s were 500 MΩ, 15 pF, and 10 MΩ, respectively: also in this case the reconstruction procedure returned an excellent concordance between the recorded and the reconstructed voltages (not shown) with very similar values of C_a and J_a. (*C*) Equivalent circuit of the "cell-PCA" system as modeled in our computer simulations. (*D*) Voltage (*a* and *c*) and current (*b* and *d*) outputs returned by the modeled Ap1D (*a* and *b*) and EPC7 (*c* and *d*) in the computer simulation of the above-described protocol (*dashed lines*), compared with the PCA outputs obtained by applying the same protocol to the real test circuit-PCA system (*dotted lines*, largely indistinguishable from the dashed lines). The stray capacitances of the test circuit were carefully measured and introduced into the model. The C_a and J_a values entered in each simulation were the same measured in the corresponding real situation, and above indicated.

ods); both the voltages and the error currents yielded by the simulations were virtually identical to those observed experimentally, as exemplified in Fig. 1 *D*. This finding confirmed the adequacy of our model in reproducing the I_Es and the voltage distortions brought about by real PCAs.

PCAs alter voltage-signal frequency components

The "cell-PCA" circuit depicted in Fig. 1 *C* can be analytically resolved, by means of Laplace transforms, for known command-current or command-voltage waveforms. Let us consider a cosinusoidal command current of frequency $\nu = \omega/2\pi$ and amplitude $I = I_{max} \cdot \cos \omega t$. Although its injection into the "unperturbed cell" would produce a membrane-voltage response of amplitude

$$V_m = (I_{max}/\omega C_m) \cdot \sin \omega t \tag{3}$$

in the perturbed situation of the "cell-PCA" system, the voltage output returned by the amplifier in response to the same current command would be

$$V_{out} = (I_{max} \cdot A/\cos \varphi) \cdot \sin(\omega t + \varphi) \tag{4}$$

where

$$A = [C_m C_a^2(1 - \omega^2 R_s J_a) + \omega^2(C_m + C_a)J_a^2]/ \{\omega[C_m^2 C_a^2(1 - \omega^2 R_s J_a)^2 + \omega^2(C_m + C_a)^2 J_a^2]\} \tag{5}$$

$$\varphi = \arctan\{-\omega(C_a^2 J_a + \omega^2 R_s C_m C_a J_a^2)/ [C_m C_a^2(1 - \omega^2 R_s J_a) + \omega^2(C_m + C_a)J_a^2]\} \tag{6}$$

This means that each frequency component of an otherwise unperturbed voltage signal would be altered by the PCA at its voltage output through a modification of its

amplitude and the introduction of a phase shift, both depending in a complex way on the frequency itself, the series resistance, and the cell capacitance. From Eqs. 3–5 it follows that the ratio of the perturbed versus unperturbed voltage frequency-component amplitude, r, would be

$$r = C_m[C_m C_a^2(1 - \omega^2 R_s J_a) + \omega^2(C_m + C_a)J_a^2]/ \{[C_m^2 C_a^2(1 - \omega^2 R_s J_a)^2 + \omega^2(C_m + C_a)^2 J_a^2]\cos\varphi\}. \quad (7)$$

As an example, we plotted the amplitude ratio, r, and the phase shift, φ, as a function of ν and for various values of C_m, for Ap1D, EPC7, and I_f-Ap200A (Fig. 2): it is worth noting that Ap1D (and, similarly, I_n-Ap200A) can either enhance or attenuate specific frequency components, by different proportions depending on C_m (and R_s), whereas EPC7 preferentially enhances the frequencies included between ~300 and 2000 Hz (again differently, depending on C_m and R_s values). Because relatively high-frequency components are markedly affected in both cases, it is expected that rapid events such as APs can be significantly altered when recorded in these conditions. The I_{fast} mode of Ap200A appears to considerably improve the amplitude and phase-shift distortions, which become of some importance only with low C_m values. Therefore, the alterations caused by I_f-Ap200A will not be thoroughly treated in the Results, and they should be considered negligible unless stated otherwise.

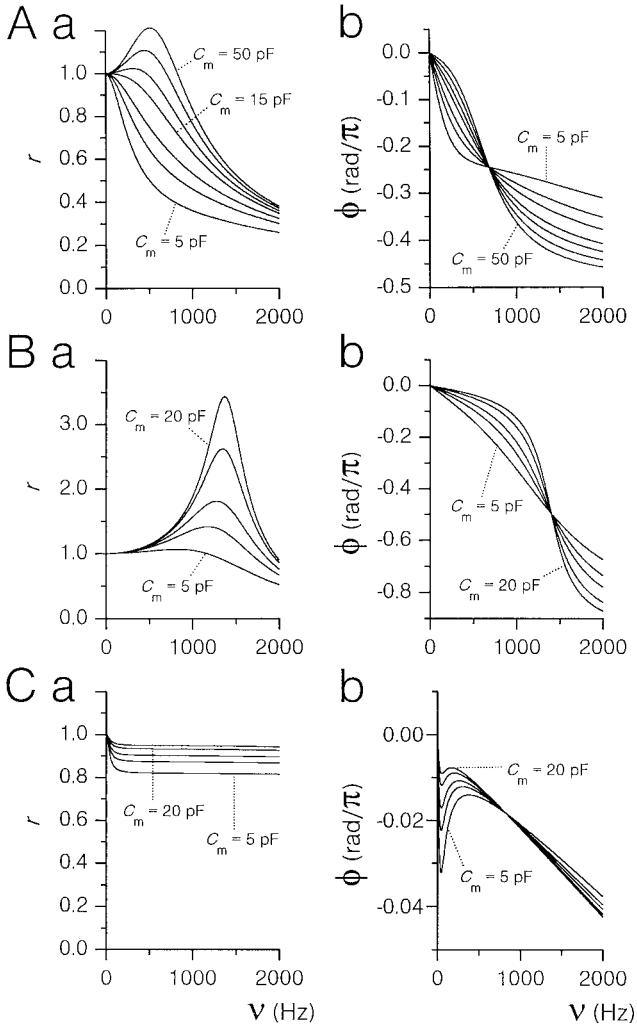

FIGURE 2 Graphics of the ratio of the PCA-perturbed versus unperturbed voltage-signal frequency-component amplitude, r (*a*), and of the PCA-generated phase shift, φ (*b*), calculated according to Eqs. 7 and 6, respectively, as a function of the frequency, ν (see text for details). Each trace corresponds to a different value of C_m. (*A*) Ap1D. C_m values are 5, 7.5, 10, 15, 20, 30, and 50 pF. (*B*) EPC7. C_m values are 5, 7.5, 10, 15, and 20 pF. (*C*) Axopatch 200A in the I_{fast} mode. C_m values are 5, 7.5, 10, 15, and 20 pF. In all cases R_s was 20 MΩ.

Simulation of the effects of PCAs used in the CC mode on cell-voltage events

The effects of PCAs working in the CC mode on cell-membrane voltage events were further investigated by numerical resolution of more complex situations. The differential equations describing the behavior of PCAs used in the CC mode (see above) were introduced into various mathematical neuronal models. The connection between the "model cell" and the "model PCA" was realized according to the scheme of Fig. 1 *C*. Each computer simulation was carried out, both excluding ("unperturbed situation") and including ("perturbed situation") the model PCA. The equations describing membrane voltage-dependent conductances were drawn from published formalizations of neuronal bioelectrical behavior (Lytton and Sejnowski, 1991; Huguenard and McCormick, 1992; McCormick and Huguenard, 1992; Bush and Sejnowski, 1994); all of the relevant cellular parameters were kept as in the original papers, except when explicitly specified otherwise (see Table 1). Other models were also tested (i.e., Hodgkin and Huxley, 1952; Traub, 1982; Rhodes and Gray, 1994); they gave essentially the same results as illustrated below, and will not be considered further in this paper. The modeled cells consisted of a single homogeneous compartment in all simulations, except those concerning equalization transients, in which a cell consisting of two compartments (according to the scheme of Fig. 7 *A*) was considered. Numeric solution of the differential equations was achieved by the use of a one-step Euler integration method. The integration step size was 15–50 μs. Preliminary tests on the adequacy of the integration method we used were carried out, either by reducing the step size by up to 100 times and checking the convergence, or by using a fourth-order Runge-Kutta integration method: both approaches confirmed that very good accuracy and stability were assured by the Euler method. The simulation programs were compiled using QuickBASIC 4.5 (Microsoft). Data were analyzed using Origin 4.0 (MicroCal).

Recordings from dorsal-root ganglion neurons

The AP off-line correction procedure (see Results) was evaluated by examining data obtained from both simulated

TABLE 1 Neuronal models used and relevant ionic-current parameters

Model no.	Reference	Specific conductances (g, nS/μm^2) and permeabilities (p, cm^3/s · μm^2)						Reversal potentials (mV)		
		g_{Na}	g_K	g_{K2}	g_A	p_T	g_{leak}	E_{Na}	E_K	E_{leak}
1	Bush and Sejnowski (1994)	0.4	0.3	0	0	0	0.8×10^{-3}*	+45	−82*	−58*
2	Lytton and Sejnowski (1991)	1.0*	0.25*	0	0.05*	0	0.8×10^{-3}*	+45*	−82*	−58*
3	Huguenard and McCormick (1992) McCormick and Huguenard (1992)	0.52*	0.07*	0	0	0	0.8×10^{-3}*	+45	−105	−58*
4	Huguenard and McCormick (1992) McCormick and Huguenard (1992)	0.41*	0.21*	0.035*	0	$0.4 \cdot 10^{-12}$*	0.8×10^{-3}*	+45	−105	−58*

*Values that have been modified from the original models. All of the equations describing voltage-dependent conductances have been maintained as in the original models.

experiments and recordings performed on real cells, namely dorsal root ganglion (DRG) neurons. The experimental procedures followed for the isolation and culturing of DRG neurons and for CC recordings were the same as described elsewhere (Wanke et al., 1994; Magistretti et al., 1996).

Sign conventions

The sign of the currents was considered with respect to the cell's interior, or to node N in the case of the passive test circuit; a current entering therein was given a negative sign. For this reason the error currents depicted in the figures are sign inverted as compared with those that would be returned (in the case of simulations) or are actually returned (in the case of real recordings) by the amplifier's current output.

RESULTS

Model PCAs distort simulated action potentials

Fast action potentials (APs) were the first physiological membrane-voltage events on which the possible alterations brought about by the model PCAs were evaluated. Fig. 3 shows examples of the effects of the model PCAs on fast spikes simulated according to published studies (Bush and Sejnowski, 1994; McCormick and Huguenard, 1992); continuous lines represent the unperturbed APs, dotted lines the APs observed, after including the PCA in the same simulation, at the voltage output of the model PCA (V_{out} of Fig. 1 *C*). It appears that Ap1D (and, similarly, I_n-Ap200A) and EPC7 can severely distort the AP shape, by delaying its upstroke; by altering its rising and falling phases, amplitude, and duration; and by modifying the afterhyperpolarization phase. Such alterations closely resemble those observed when comparing APs recorded using either a PCA or a classical bridge amplifier in real neurons (for instance, compare Fig. 3 *Aa* with figure 1 *A–C* in Magistretti et al., 1996, or with Fig. 8 *Ba* of the present work). The model PCAs also generated and conducted error currents (I_Es) similar to those returned by the PCA I_{out} when real APs are recorded (Figs. 3, *Ab* and *Bb*, and 8 *Bb*). The effects of PCAs on the main AP shape parameters are summarized in Table 2. The AP amplitude was normally augmented by PCAs, so that the reversal potential of sodium currents was easily exceeded. The AP upstroke was slowed down by Ap1D, and could be either slightly slowed down (see Fig. 3 *Ba*) or accelerated (see below) by EPC7. Both Ap1D and (more pronouncedly) EPC7 accelerated the AP repolarization phase. The AP duration was markedly decreased by EPC7, whereas it was normally little affected (Fig. 3 *A*) or increased (see below) by Ap1D. Under some circumstances, rapid oscillations and, evidently, unphysiological alterations were generated by EPC7; that is why two different sets of

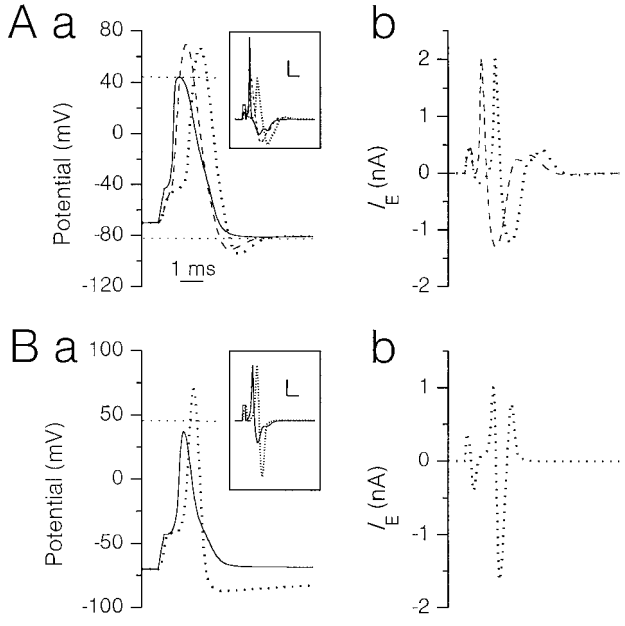

FIGURE 3 Simulations of the effects of PCAs on single APs. (*A*) Ap1D. (*a*) Unperturbed AP (*continuous line*) and PCA-perturbed AP in normal conditions (*dotted line*). The dashed line is the PCA-perturbed AP obtained by commanding the unperturbed time-dependent variations of membrane voltage-dependent conductances. The horizontal dotted lines mark the reversal potentials for Na^+ and K^+ currents. The traces in the inset are the time derivatives of the corresponding voltage traces (calibration bars: 100 V·s^{-1}, 1 ms). (*b*) PCA-generated error currents. Dotted and dashed lines: as above. The model used was no. 1. C_m = 12.6 pF, R_s = 20 MΩ, T = 34°C. (*B*) EPC7. (*a*) Unperturbed AP (*continuous line*) and PCA-perturbed AP (*dotted line*). The horizontal dotted line marks the reversal potential for Na^+ currents. (*Inset*) As in *A*. (*b*) PCA-generated error current. The model used was no. 3. C_m = 6.2 pF, R_s = 12 MΩ, T = 34°C. In all cases, the AP was elicited by injecting a 255-μs current pulse of +100 pA/pF (I_{com}) into C_m, from a resting membrane potential (rmp) of −70 mV.

TABLE 2 Alterations of AP shape parameters generated by PCAs

	DR_{max} (pert./contr.)	RT_{10-90} (pert./contr.)	Amplitude (pert./contr.)	RR_{max} (pert./contr.)	Duration (pert./contr.)	Extra hyperpolarization (mV)
Ap1D	0.54	1.79	1.3	1.57	0.96	−9.9
EPC7	0.99	1.31	1.42	2.52	0.83	−18.6

The APs illustrated in Fig. 3, *Aa* and *Ba* (*continuous and dotted lines*), have been used for obtaining exemplary values of AP shape parameters. The following parameters have been considered: maximum AP depolarization rate (DR_{max}), rise time 10–90% (RT_{10-90}), AP amplitude (measured from the AP threshold), maximum AP repolarization rate (RR_{max}), AP duration (measured in correspondence with the AP half-amplitude). The values obtained from the perturbed APs have been normalized to the corresponding ones of the control APs (pert./contr.). Also indicated are the amplitudes of the perturbed APs' extra hyperpolarizations, which were derived by measuring the most negative voltage value subsequent to an AP and subtracting the value of the control AP from that of the corresponding perturbed AP.

simulation parameters are used in Fig. 3 to exemplify the effects of Ap1D and EPC7.

Another prominent effect of the model PCAs was an exaggeration of the hyperpolarization following the AP, which was often such as to produce pronounced, spurious afterhyperpolarizations; these afterhyperpolarizations could even exceed the potassium reversal potential (E_K) (see Fig. 3 *Aa*).

Interestingly, our data indicate that the AP amplitude can be increased by PCAs, even under conditions in which no frequency-component enhancement would be expected, on the basis of the simplified situation of an externally applied command current described in the Methods and Theory (compare Fig. 3 *Aa* with Fig. 2 *Aa*). This implies that in the case of a firing cell, additional error sources contribute to the observed alterations. Two factors can be taken into account as possible candidates: 1) PCA-generated V_m distortions significantly alter the driving forces for membrane ionic currents, thereby modifying the development of the currents themselves; 2) PCA-generated V_m distortions alter the normal interaction between V_m and voltage-dependent conductances. To discriminate between the relative contributions of these two possible error sources, we performed the same simulations on single spikes seen above, with the difference that the time courses of voltage-dependent conductances were externally imposed and kept equal to those taking place in the unperturbed situation: under these conditions no contribution at all of the latter above-mentioned factor is possible. Fig. 3 *Aa* (*dashed line*) shows that also in this case, the model PCA can produce alterations of the AP shape similar to the previously described ones, although they appear to be slightly different quantitatively and the AP delay is reduced. This finding suggests that alterations of ionic-current driving forces are a major element in determining PCA-generated AP distortions, and that interferences with the voltage and time dependence of membrane voltage-operated conductances can give a further contribution.

Effects of cellular and experimental parameters on PCA-generated action-potential distortions

Equations 6 and 7 show that the alterations caused by PCAs on membrane-voltage events critically depend on C_m and R_s. Therefore we tested the effects of varying both parameters on the importance of PCA-generated distortions of APs. As shown in Fig. 4 *Aa* and *b*, increasing R_s values normally resulted in a moderate aggravation of PCA-driven AP alterations, which, on the other hand, remained qualitatively similar: the most R_s-sensitive parameters were AP duration and depolarization rate in the case of Ap1D, and AP amplitude and repolarization rate in the case of EPC7. Of special interest is the observation that significant distortions can be produced by PCAs with R_s values as low as 5 MΩ (Fig. 4 *A*).

Variations of C_m proved to markedly affect AP distortions (Fig. 4, *Ba* and *b*). In the case of Ap1D, the most prominent effects of reducing C_m from 30 to 5 pF were a progressive increase in AP duration, a further decrease in the AP depolarization rate, and a dramatic exaggeration of the spurious afterhyperpolarization. In the case of EPC7, the generation of a prolonged, spurious afterhyperpolarization was also a major effect of reducing C_m from 17 to 5 pF, whereas increasing C_m led to a slight increase in the AP depolarization rate and a further decrease in AP duration. The remaining AP shape alterations were mildly attenuated by lowering C_m values in both PCAs.

The effects of temperature (T) variations on APs during recordings with PCAs were also evaluated, to indirectly test the importance of the rapidity of a cell-voltage event in determining PCA-driven distortions upon it. Raising T (from 28°C to 37°C) and thus accelerating the AP progressively enhanced the main alterations brought about by the PCAs: depolarization rate decrease and generation of spurious afterhyperpolarizations, in the case of Ap1D (a progressive AP duration increase was an additional effect); augmentation of the AP amplitude and repolarization rate, and generation of spurious afterhyperpolarizations, in the case of EPC7 (not shown).

Effects of PCAs on repetitive firing frequency

From all of the above-illustrated instances of simulated APs, it turns out that PCAs can markedly alter the repolarization phase and generate spurious afterhyperpolarizations, which are often profound and/or prolonged. Such distortions may be expected to interfere with an otherwise unperturbed

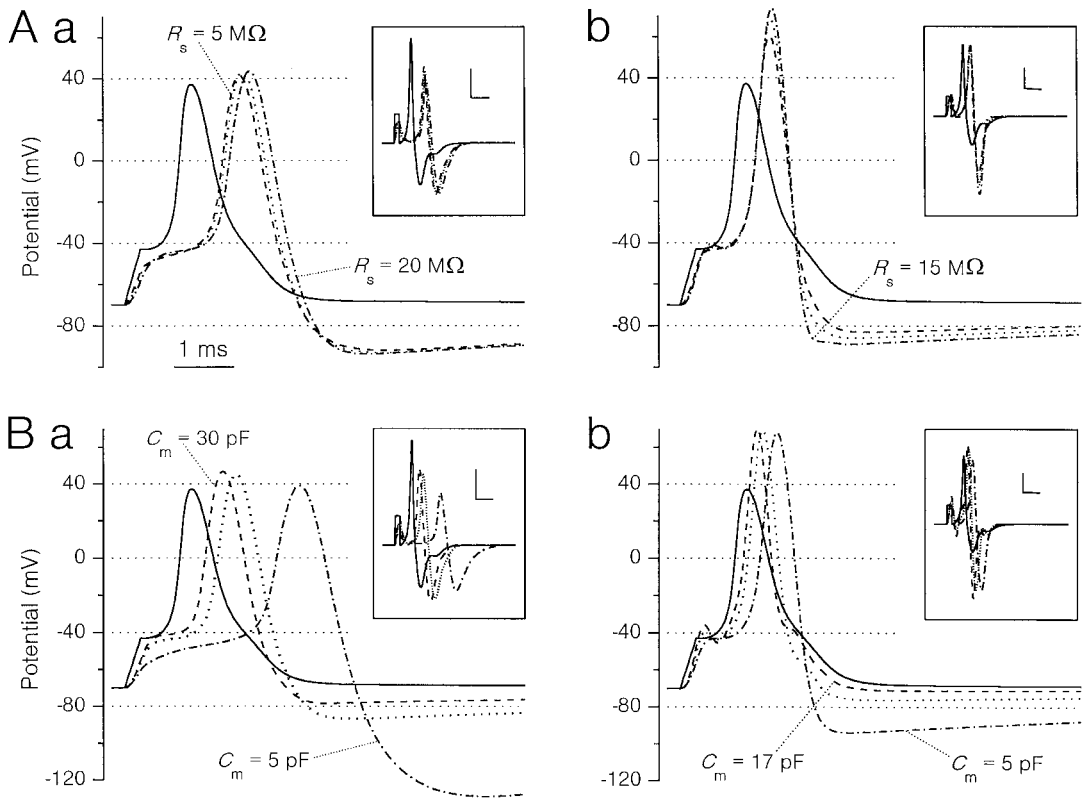

FIGURE 4 Simulations of the influence of R_s and C_m on PCA-generated distortions of single APs. Continuous lines represent the unperturbed APs in all panels. The model used was no. 3 throughout. (*A*) Effects of R_s. (*a*) Ap1D. R_s = 5 MΩ (*dashed line*), 10 MΩ (*dotted line*), and 20 MΩ (*dashed/dotted line*). C_m = 12.6 pF, T = 34°C. (*b*) EPC7. R_s = 5 MΩ (*dashed line*), 10 MΩ (*dotted line*), and 15 MΩ (*dashed/dotted line*). C_m = 6.2 pF, T = 34°C. (*B*) Effects of C_m. (*a*) Ap1D. C_m = 30 pF (*dashed line*), 17 pF (*dotted line*), and 5 pF (*dashed/dotted line*). R_s = 15 MΩ, T = 34°C. (*b*) EPC7. C_m = 17 pF (*dashed line*), 10 pF (*dotted line*), and 5 pF (*dashed/dotted line*). R_s = 10 MΩ, T = 34°C. The traces in the inset of each panel are the time derivatives of the corresponding voltage traces (calibration bars: 100 V · s^{-1}, 1 ms). The command current pulses were the same as in Fig. 3.

regular discharge of APs. We verified this possibility by simulating the effects of PCAs on various models of neuronal repetitive firing (Lytton and Sejnowski, 1991; McCormick and Huguenard, 1992; Bush and Sejnowski, 1994).

The results we found were different, depending on the model used and the parameters introduced therein. Fig. 5 shows that the firing frequency was not affected by the simulated Ap1D when the model by Bush and Sejnowski (1994) was employed, but it was in the case of those by Lytton and Sejnowski (1991) and by McCormick and Huguenard (1992). The factor that turned out to be especially important in this respect is the deactivation speed of the repolarizing potassium current(s). A profound, PCA-driven spurious afterhyperpolarization would tend to deactivate the voltage-dependent potassium conductances activated during the AP to a higher extent than would occur in the unperturbed situation: if the deactivation rate is slow (as in Bush and Sejnowski, 1994), the membrane time constant (τ_m), decreased by the activation of these conductances, will remain fast for a sufficiently long period to allow V_m to return quickly to unperturbed values, once the approaching of V_m to E_K has curtailed the outward currents (Fig. 5 *A*); if the deactivation rate is fast (as in Lytton and Sejnowski, 1991, and McCormick and Huguenard, 1992), τ_m will rapidly recover to the resting value, and V_m will rise back according to this value. In the latter case, if the resting τ_m is sufficiently high (as in the original models), the subsequent AP's firing can be considerably delayed, and therefore the firing frequency can be significantly lowered (Fig. 5 *Ba*, *C*); if, on the other hand, τ_m is lower, the subsequent AP's firing can be unaffected or even anticipated, because of a prompter hyperpolarization-driven recovery of sodium channels from inactivation; the firing frequency can thus be also increased (Fig. 5 *Bb*). Very similar results were observed in the case of EPC7, when the parameters introduced in the models were such as to induce significant spurious afterhyperpolarizations (see Fig. 5 *D*). These data show that the two PCAs can unpredictably affect repetitive firing in different cell systems.

Fig. 2 *Ca* shows that I_f-Ap200A can significantly attenuate the amplitude of voltage signals, even in their low-frequency components (from ~50 Hz upwards), provided that C_m is sufficiently low. As a consequence, I_f-Ap200A can be expected to artifactually reduce the firing frequency in low-capacitance cells. This was confirmed by simulating such a situation, as exemplified in Fig. 5 *E*.

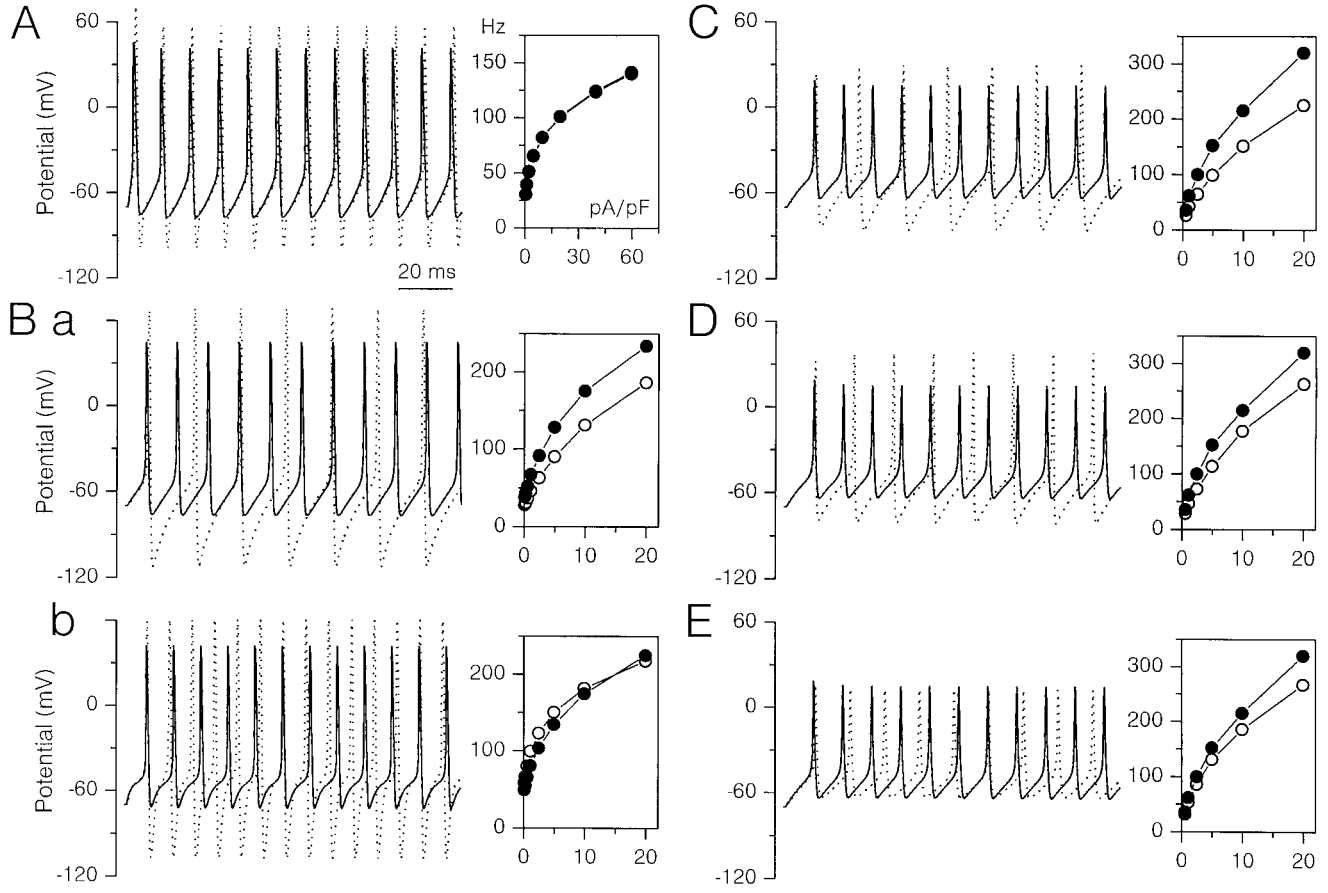

FIGURE 5 Simulations of the effects of PCAs on rhythmic firing. Continuous lines and dotted lines represent the unperturbed and the perturbed firing, respectively, in all panels. The AP firing was evoked by injecting depolarizing current pulses of various amplitude into C_m, from a rmp of −70 mV. (*A*) Effect of Ap1D on the firing generated by model no. 1. (*B*) Effect of Ap1D on the firing generated by model no. 2. τ_m was 12.5 ms in *a*, and 1.25 ms in *b*. (*C*) Effect of Ap1D on the firing generated by model no. 3. In *A*, *B*, and *C*, C_m was 8.0 pF and R_s was 20 MΩ. (*D*) Effect of EPC7 on the firing generated by model no. 3. C_m was 6.2 pF and R_s was 10 MΩ. (*E*) Effect of Axopatch 200A in the I_{fast} mode on the firing generated by model no. 3. C_m was 6.2 pF and R_s was 15 MΩ. *T* was 34°C in all cases. The inset of each panel is the graphic of the firing frequency (in Hz) as a function of the current-pulse amplitude (in pA/pF) in the corresponding model, both in the unperturbed (*filled symbols*) and in the perturbed (*empty symbols*) situation.

Effects of PCAs on low-threshold spikes and burst firing

Effects of PCAs similar to those illustrated in the previous paragraph may be expected when APs are generated in groups by an underlying transient voltage event like a low-threshold spike (LTS), rather than in trains by step-current injection. This assumption was verified by simulating a burst firing according to the model of McCormick and Huguenard (1992), in which the burst is sustained by a LTS due to the recruitment of a low-threshold, T-type calcium current. The results are exemplified in Fig. 6. Similar to what is seen in the case of the repetitive firing obtained from the same model (Fig. 5 *C*), the APs within a burst were delayed by the simulated Ap1D. If the T-current density was reduced to decrease the LTS duration and to produce a burst made of just two spikes, the PCA-generated distortions prevented the firing of the second AP (Fig. 6 *B*). In a similar real situation, the bursting nature of a neuron might therefore be missed.

Ap1D had no significant effects on the shape of the LTS underlying the burst, as examined by setting the maximum sodium conductance to zero (not shown); this was expected, because of the relative slowness of such a membrane-voltage event. Effects qualitatively similar to those seen for Ap1D were brought about by EPC7 (not shown).

Effects of PCAs on fast time constants

Measurements of τ_ms lying within the physiological range are unlikely to be significantly altered when performed on data obtained with PCAs. However, much faster time constants are also present in voltage transients evoked in geometrically complex cells, as a consequence of charge movements between nonequipotential, distinct membrane regions. Exact knowledge of the values of such time constants (equalization time constants, τ_{eq}s) is important for gaining insight into the electrotonic structure of a given

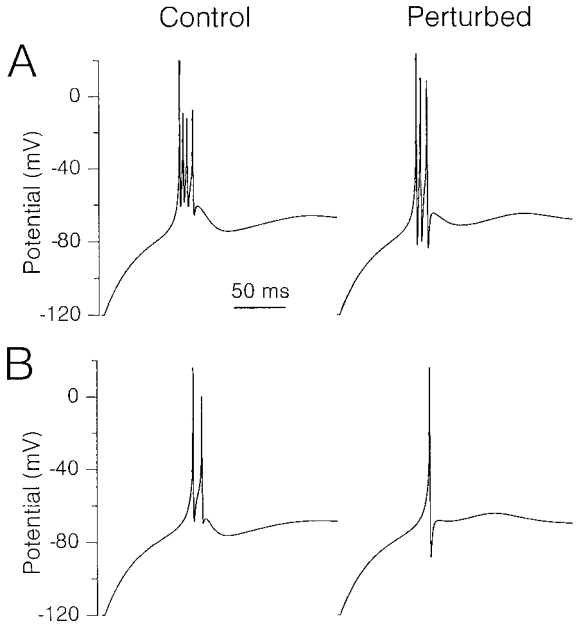

FIGURE 6 Simulations of the effects of Ap1D on burst firing. The model used was no. 4. (*A*) Simulation of a rebound burst generated when the command current injected to keep the rmp at −120 mV was stepped to zero. (*B*) The maximum permeability of the low-voltage activated calcium current was lowered to 0.21×10^{-12} cm^3/s · μm^2 to reduce the number of APs in the burst. C_m = 12.6 pF, R_s = 20 MΩ, T = 35°C in both cases.

neuronal type (for the application of τ_{eq}s to the determination of neuronal electrotonic length on the basis of the cable theory, see Rall, 1969, 1977). A common procedure for the measurement of τ_{eq}s consists of the injection of a very brief but strong current pulse able to generate a measurable off-response transient: in a geometrically complex cell the decay of this transient is determined by both τ_{eq}s and τ_m, and the τ_{eq} values are completely independent of the command-pulse duration. We reproduced a similar protocol in a two-compartment cell model (see Fig. 7 *A*), in the absence or presence of the simulated PCAs. We found that the ensuing voltage transients could be markedly distorted in their early phases by PCAs, and that the alterations depended quantitatively and qualitatively on a number of variables, including R_s, compartment membrane capacitance, compartment membrane conductance, intercompartmental resistance, command-pulse duration, and command-pulse amplitude. Measurements of τ_{eq} from such experimental outputs would therefore be variably altered. Fig. 7 (*B* and *C*) shows a few examples of the modifications produced by simulated Ap1D and EPC7 on equalization voltage transients, under diverse conditions. The transients obtained with recordings made using Ap1D can return spurious τ_{eq} values either higher or lower than the real ones, depending on the above-mentioned parameters (Fig. 7, *Ba* and *b*); recordings made with EPC7 will preferentially return abnormally faster τ_{eq}s (Fig. 7 *C*). In either case, τ_ms appear to be essentially unaffected.

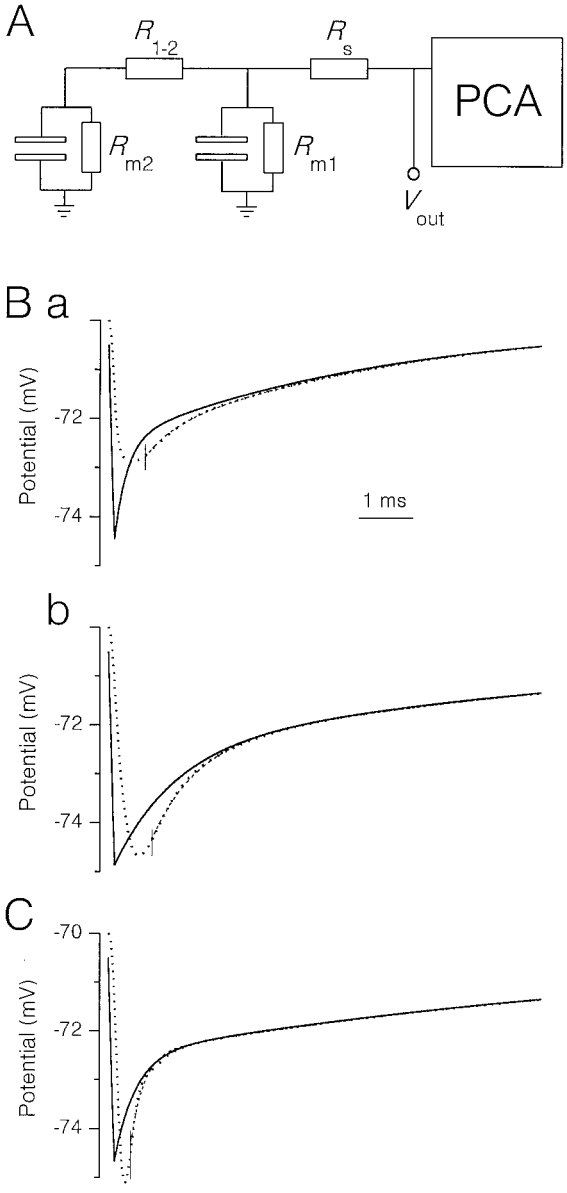

FIGURE 7 Simulations of the effects of PCAs on passive voltage transients in a two-compartment cell model. (*A*) Equivalent circuit of the two-compartment cell model. The membrane time constant, τ_m, was assumed equal in both compartments. (*B, C*) Effects of PCAs on passive transients evoked by 125-μs current pulses of −20 pA/pF. Continuous lines are the unperturbed transients, dotted lines are the perturbed transients, dashed lines (largely indistinguishable from the former ones) are biexponential best fittings. The vertical bars mark the beginning of the fitted trace portion. (*B*) Ap1D. (*a*) Passive transients in a model cell with τ_m = 5 ms, $R_{m1} = R_{m2}$ = 0.5 GΩ, R_{1-2} = 50 MΩ, R_s = 10 MΩ. Fitting parameters were A_1 = −1.99 mV, τ_1 = 0.232 ms, A_2 = −2.47 mV, τ_2 = 5.0 ms, A_0 = −70.0 mV (unperturbed); A_1 = −0.507 mV, τ_1 = 0.49 ms, A_2 = −2.3 mV, τ_2 = 4.9 ms, A_0 = −70.0 mV (perturbed). (*b*) Passive transients in a model cell with τ_m = 12.5 ms, $R_{m1} = R_{m2}$ = 0.5 GΩ, R_{1-2} = 100 MΩ, R_s = 20 MΩ. Fitting parameters were A_1 = −2.38 mV, τ_1 = 1.13 ms, A_2 = −2.49 mV, τ_2 = 12.5 ms, A_0 = −70.0 mV (unperturbed); A_1 = −1.9 mV, τ_1 = 0.816 ms, A_2 = −2.45 mV, τ_2 = 11.91 ms, A_0 = −70.0 mV (perturbed). (*C*) EPC7. The passive transients were evoked in a model cell with τ_m = 12.5 ms, $R_{m1} = R_{m2}$ = 1.5 GΩ, R_{1-2} = 100 MΩ, R_s = 10 MΩ. Fitting parameters were A_1 = −2.18 mV, τ_1 = 0.397 ms, A_2 = −2.49 mV, τ_2 = 12.5 ms, A_0 = −70.0 mV (unperturbed); A_1 = −1.9 mV, τ_1 = 0.243 ms, A_2 = −2.47 mV, τ_2 = 12.2 ms, A_0 = −70.0 mV (perturbed).

Off-line corrections: are they feasible?

It has previously been shown that in the simplified experimental situation of a passive test circuit, the voltage distortions brought about by PCAs can be corrected off-line by exploiting the I_E signal returned by PCAs themselves (Magistretti et al., 1996): in this case, both a "resistive" and a "capacitive" error term can be calculated from I_E and added to the perturbed voltage trace, thus correcting the distortions. The appropriateness of this approach under the same conditions was confirmed by our simulations (Fig. 8 *A*).

However, the existence of limitations for the off-line correction became evident when this procedure was tested on real AP recordings made with PCAs. Fig. 8 *B* shows the result returned by the correction for an AP recorded in a DRG neuron using the Ap1D amplifier. The shape of the "corrected" AP was far from that of an unperturbed AP (recorded with a classical voltage follower), and the distortions appeared to be accentuated rather than reduced.

A major requisite for the success of the off-line correction is that the total resistive current flowing through R_{inj} (in the case of the passive test circuit: I_{inj}) or through the cell membrane (in the case of a single-compartment cell model) is essentially the same in the perturbed situation as in the unperturbed one; this is because this current is the sum of the actual capacitive current, I_{Cp}, and I_E, and therefore corresponds to the total current "commanded" into C_m after the off-line correction has been carried out. This requirement is indeed met in the tests performed in the simplified situation of the passive test circuit (see Fig. 8 *Ab*). The question then arises whether the same can also be considered to be true in the more complex situation of a firing cell.

In Fig. 8 *Cb* the total resistive currents flowing through the membranes of an unperturbed cell (I_{Ru}) and a PCA-perturbed cell (I_{Rp}) during a simulated AP are compared. The two currents still appear to be strikingly different; therefore the above condition for successfully performing an off-line correction here no longer holds. This conclusion is confirmed by the comparison of the simulated, unperturbed AP with the "corrected" one (Fig. 8 *Ca*). Marked discrepancies between I_{Rp} and I_{Ru} were also observed when the time courses of voltage-dependent conductances were externally fixed, as explained above (first paragraph of the Results) (not shown). These findings demonstrate that the voltage distortions generated by PCAs during an AP both alter the membrane ionic-current driving forces and interfere with the normal interaction between V_m and voltage-dependent conductances, thereby irremediably changing the current flow across the whole circuit and precluding the possibility of an off-line correction.

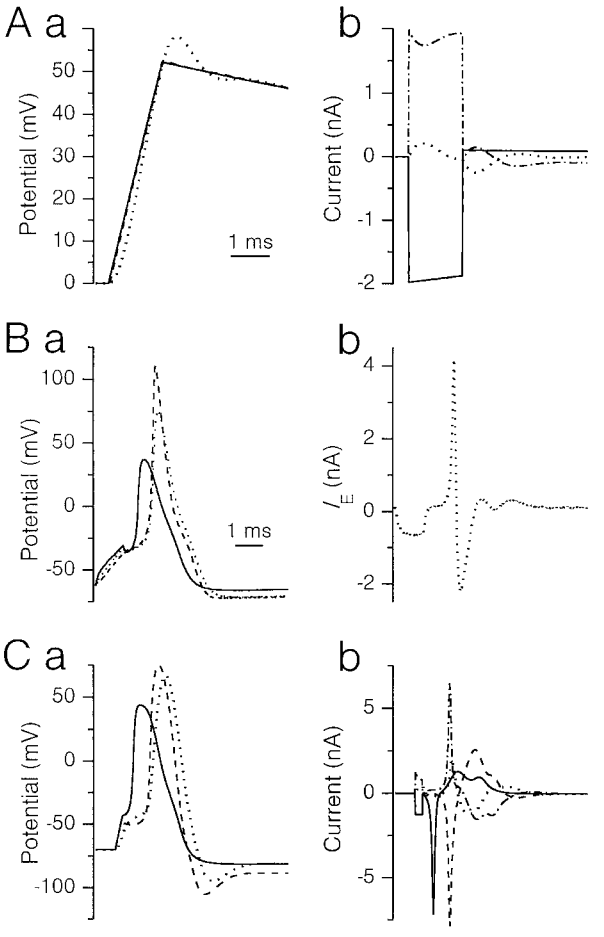

FIGURE 8 Evaluation of the results of the off-line correction procedure. (*A*) Off-line correction performed on the traces returned by simulating an experiment on a test circuit-PCA system. The test circuit and PCA modeled and the protocol applied were the same as in Fig. 1 *Da*, *b*, save that the test-circuit stray capacitances were omitted. (*a*) Unperturbed voltage (*continuous line*), perturbed voltage (*dotted line*), and corrected voltage (*dashed line*). (*b*) Unperturbed I_{inj} (*continuous line*), I_E (*dotted line*), I_{Cp} (*dashed-dotted line*), and perturbed I_{inj} (*dashed line*) (see text for details). (*B*) Off-line correction performed on a real AP recorded using an Ap1D amplifier from a cultured DRG neuron. (*a*) The continuous line is the unperturbed AP, recorded with a classical voltage follower (Axoclamp 2A amplifier); the dotted line is the AP derived, from the same cell, using Ap1D; and the dashed line is the "corrected" AP. (*b*) The error current, I_E, returned by the Ap1D current output, and used for the correction procedure. (*C*) Off-line correction performed on a simulated AP. The model cell-PCA system and the protocol applied were the same as in Fig. 3 *A*. (*a*) Unperturbed AP (*continuous line*), perturbed AP (*dotted line*), and "corrected" AP (*dashed line*). (*b*) $I_{Ru} + I_{com}$ (*continuous line*), I_E (*dotted line*), I_{Cp} (*dashed-dotted line*) and $I_{Rp} + I_{com}$ (*dashed line*) (see text for details).

DISCUSSION

The electronic design of conventional PCAs, which has been extensively discussed elsewhere (Sigworth, 1995; Magistretti et al., 1996), was originally conceived for voltage-clamp recordings with low-resistance electrodes. Turning PCAs to the CC mode requires the introduction of additional feedback circuits that compensate a basically very low resistance of the PCA input stage. Because this circuitry provides a positive feedback loop, its reaction speed cannot be infinitely high; on the contrary, it must be limited, otherwise signal instabilities and fast oscillations would be generated. Therefore, the performance of the feedback circuitry, which is satisfactory for relatively low frequency components of the signal, may be inadequate at

higher frequencies; as a consequence, signal-frequency-dependent error currents, I_E, are produced. As we have previously demonstrated, these currents, flowing through the PCA, generate distortions in the voltage signals returned by the PCA itself.

The primary goal of the present study was to collect data allowing us to predict which cell membrane voltage events are especially affected in CC recordings made with PCAs, and which cellular parameters and experimental conditions can aggravate, or conversely attenuate, PCA-generated distortions. Such information is desirable in view of a more rational use of PCAs in future experiments and the requirement of a critical review of the published literature. The strategy we chose was to determine the CC voltage-I_E transfer function for the different PCA models considered. These functions were then used, on one hand, to analytically derive general equations describing the effects caused by PCAs, under simplified experimental conditions, on voltage-signal frequency components, and on the other hand, to create corresponding models of PCA functioning that were introduced into numerical simulations of neuronal bioelectrical behavior. In this way we were able to evaluate a variety of experimental and physiological situations. In particular, the modeling approach showed that rapid membrane voltage events such as fast action potentials are preferentially altered by PCAs, consistent with what was previously observed in real cells (Magistretti et al., 1996). Fine AP shape parameter measurements made on recordings obtained using PCAs such as List EPC-7, Axopatch 1D, or Axopatch 200A, working in the I_{normal} mode, can be affected by severe alterations. For example, in such conditions it would be improper to try to estimate the sodium channel density from the maximal slope of the AP upstroke, or to consider a cell "healthy" because of a high AP amplitude. Another striking effect of model PCAs was the generation of prominent, artifactual afterhyperpolarizations, again in accordance with experimental data (Magistretti et al., 1996). Because the ability to produce afterhyperpolarizations, one of the basic bioelectrical properties of neuronal membranes, is differently expressed and has different patterns and functional implications in different neuronal populations (Schwindt et al., 1988; Sah and McLachlan, 1992; Sah, 1996), the presence of spurious or distorted afterhyperpolarizations may lead to erroneous conclusions as to their importance and physiological role.

Various cellular and experimental parameters turned out to be able to affect the entity of PCA-generated distortions. A first factor is the cell-to-amplifier access resistance, R_s; our results indicate that, in general, the presence of low R_s values attenuates the artifacts. However, the importance of R_s does not appear to be determinant, because the attenuation of distortions obtained by lowering R_s was only partial, and significant alterations were still present with R_s values as low as 5 MΩ. The latter observation gains further importance from the fact that PCAs of more recent generations (i.e., Axopatch 200A, Axopatch 200B) provide an I_{fast} mode that greatly improves the reliability of CC recordings (see Magistretti et al., 1996, and this work), but is stable only with R_s values higher than 5–10 MΩ. Therefore, under conditions in which the I_{fast} mode could not be used—namely with a low R_s, which is especially desirable when concomitant voltage-clamp/current-clamp recordings are performed—prominent alterations would still be possible.

Cell capacitance, C_m, proved to be an important factor in influencing the entity of PCA-generated distortions (see Results). Some of these artifacts can become dramatic in the presence of very low C_ms, as in the case of spurious afterhyperpolarizations. Aggravations of the major alterations brought about by each PCA model are also to be expected as a consequence of temperature increases.

Our study also revealed that such membrane-voltage events as regular firing and burst firing cannot be assumed to be free of problems when recorded with PCAs. In the presence of particular kinetic properties of the underlying voltage-dependent currents (see Results), the firing frequencies of a neuron may be underestimated or, alternatively, overestimated, depending on the passive characteristics of the neuron itself. As a consequence of firing-frequency-dependent alterations in the interspike interval (see Fig. 5, *insets*), the process of adaptation might also be interfered with.

Additional rapid membrane-voltage events that can be experimentally revealed in neurons, and which derive from charge movements across distinct neuronal compartments, are equalization transients. Our data indicate that PCA-generated distortions can significantly alter the measurement of equalization time constants, and, consequently, the estimation of a neuron's electrotonic structure. Hence, for deriving reliable measurements of neuronal electrotonic parameters from experiments performed with conventional PCAs, data obtained under voltage-clamp conditions should rather be used, following the method indicated by Jackson (1992).

Another major aim of the present work was to test the feasibility of off-line corrections of the voltage signals obtained with PCAs, by exploiting the I_E signals returned by the PCA current output. Both the results of the model and the recordings obtained from real neurons demonstrated that such a possibility should be ruled out. Our simulations also revealed that this is the consequence of a global alteration, caused by the PCA functioning, of the currents flowing through the cell membrane-PCA system. This finding, together with others previously discussed, point to the importance of modifying the functioning principles and electronic design of the CC mode of conventional PCAs. In a previous paper (see Magistretti et al., 1996) we have already proposed a possible electronic solution that would make CC recordings performed with PCAs as reliable as those obtained with classical voltage followers, thus overcoming all of the problems and limitations that we have described here.

In conclusion, our results indicate that the use of such PCAs as Axopatch 1D and List EPC-7 for CC recordings is appropriate only under particular experimental conditions, for instance, when slow membrane-voltage signals

(postsynaptic potentials, slow regenerative potentials, etc.) are to be investigated, or when the cells under study are large. The above-discussed limitations of conventional PCAs as a tool for performing CC recordings make it necessary to preliminarily select the specific cases in which these instruments can safely be used for studying cell-voltage events, and/or to carefully evaluate a posteriori the experimental situations encountered each time.

REFERENCES

Bielefeldt, K., and M. B. Jackson. 1993. A calcium-activated potassium channel causes frequency-dependent action-potential failures in a mammalian nerve terminal. *J. Neurophysiol.* 70:284–298.

Bush, P. C., and T. J. Sejnowski. 1994. Effects of inhibition and dendritic saturation in simulated neocortical pyramidal cells. *J. Neurophysiol.* 71:2183–2193.

D'Angelo, E., G. De Filippi, P. Rossi, and V. Taglietti. 1995. Synaptic excitation of individual rat cerebellar granule cells in situ: evidence for the role of NMDA receptors. *J. Physiol. (Lond.).* 484.2:397–413.

D'Angelo, E., P. Rossi, and V. Taglietti. 1993. Different proportions of *N*-methyl-D-aspartate and non-*N*-methyl-D-aspartate receptor currents at the mossy fibre-granule cell synapse of developing rat cerebellum. *Neuroscience.* 53:121–130.

Gryder, D. E., and D. A. Coulter. 1996. Patch clamp recordings of hippocampal alvear/oriens inhibitory interneuron activity during electrographic seizures. *Soc. Neurosci. Abstr.* 22:2098.

Hodgkin, A. L., and A. F. Huxley. 1952. A quantitative description of membrane current and its application to conduction and excitation in nerve. *J. Physiol. (Lond.).* 117:500–549.

Huguenard, J. R., and D. A. McCormick. 1992. Simulation of the currents involved in rhythmic oscillations in thalamic relay neurons. *J. Neurophysiol.* 68:1373–1383.

Jackson, M. B. 1992. Cable analysis with the whole-cell patch mode. Theory and experiment. *Biophys. J.* 61:756–766.

Johansson, S., W. Friedman, and P. Århem. 1992. Impulses and resting membrane properties of small cultured rat hippocampal neurons. *J. Physiol. (Lond.).* 445:129–140.

Kawaguchi, Y. 1993. Groupings of nonpyramidal and pyramidal cells with specific physiological and morphological characteristics in rat frontal cortex. *J. Neurophysiol.* 69:416–431.

Lytton, W. W., and T. J. Sejnowski. 1991. Simulation of cortical pyramidal neurons synchronized by inhibitory interneurons. *J. Neurophysiol.* 66: 1059–1079.

Magistretti, J., M. Mantegazza, E. Guatteo, and E. Wanke. 1996. Action potentials recorded with patch-clamp amplifiers: are they genuine? *Trends Neurosci.* 19:530–534.

McCormick, D. A., and J. R. Huguenard. 1992. A model of electrophysiological properties of thalamocortical relay neurons. *J. Neurophysiol.* 68:1384–1400.

Pape, H.-C., T. Budde, R. Mager, and Z. F. Kisvarday. 1994. Prevention of Ca^{2+}-mediated potentials in GABAergic local circuit neurones of rat thalamus by a transient K^+ current. *J. Physiol. (Lond.).* 478.3:403–422.

Rall, W. 1969. Time constants and electrotonic length of membrane cylinders and neurons. *Biophys. J.* 9:1483–1508.

Rall, W. 1977. Core conductor theory and cable properties of neurones. *In* Handbook of Physiology. The Nervous System, Vol. I. American Physiological Society, Bethesda, MD. 81–90.

Rhodes, P. A., and C. M. Gray. 1994. Simulation of intrinsically bursting neocortical pyramidal neurons. *Neural Computation.* 6:1086–1110.

Sah, P. 1996. Ca^{2+}-activated K^+ currents in neurones: types, physiological roles and modulation. *Trends Neurosci.* 19:150–154.

Sah, P., and E. M. McLachlan. 1992. Potassium currents contributing to action potential repolarization and the afterhyperpolarization in rat vagal motoneurons. *J. Neurophysiol.* 68:1834–1841.

Schwindt, P. C., W. J. Spain, R. C. Foehring, C. E. Stafstrom, M. C. Chubb, and W. E. Crill. 1988. Multiple potassium conductances and their functions in neurons from cat sensorimotor cortex in vitro. *J. Neurophysiol.* 59:424–449.

Sciancalepore, M., and A. Constanti. 1995. Patch-clamp study of neurones in rat olfactory cortex slices: properties of a slow post-stimulus afterdepolarizing current (I_{ADP}). *NeuroReport.* 6:2489–2494.

Sigworth, F. J. 1995. Electronic design of the patch clamp. *In* Single-Channel Recording. B. Sakmann and E. Neher, editors. Plenum Press, New York and London. 95–127.

Sontheimer, H., J. A. Black, B. R. Ransom, and S. G. Waxman. 1992. Ion channels in spinal chord astrocytes in vitro. I. Transient expression of high levels of Na^+ and K^+ channels. *J. Neurophysiol.* 68:985–1000.

Stern, P., F. A. Edwards, and B. Sakmann. 1992. Fast and slow components of unitary EPSCs on stellate cells elicited by focal stimulation in slices of rat visual cortex. *J. Physiol. (Lond.).* 449:247–278.

Traub, R. D. 1982. Simulation of intrinsic bursting in CA3 hippocampal neurons. *Neuroscience.* 7:1233–1242.

Wanke, E., L. Bianchi, M. Mantegazza, E. Guatteo, E. Mancinelli, and A. Ferroni. 1994. Muscarinic regulation of Ca^{2+} currents in rat sensory neurons: channel and receptor types, dose-response relationship and cross-talk pathways. *Eur. J. Neurosci.* 6:381–391.

Zhang, L., and C. J. McBain. 1995. Potassium conductances underlying repolarization and after-hyperpolarization in rat CA1 hippocampal interneurones. *J. Physiol. (Lond.).* 488.3:661–672.